Carbohydrate Polymers 117 (2015) 279–285

Contents lists available at ScienceDirect

Carbohydrate Polymers

journal homepage: www.elsevier.com/locate/carbpol

# Physical characterisation of high amylose maize starch and acylated high amylose maize starches

Ya-Mei Lim[a,b,c], Pamela Hoobin[d], DanYang Ying[a], Iko Burgar[d], Paul R. Gooley[b,c,*], Mary Ann Augustin[a]

[a] CSIRO Preventative Health National Research Flagship & Animal, Food and Health Sciences, 671 Sneydes Road, Werribee, Melbourne 3030, VIC, Australia
[b] Department of Biochemistry and Molecular Biology, The University of Melbourne, Parkville, Melbourne 3010, VIC, Australia
[c] The Bio21 Molecular Science and Biotechnology Institute, The University of Melbourne, Parkville, Melbourne 3010, VIC, Australia
[d] CSIRO Manufacturing & Materials Technology, Private Bag 33, Clayton South MDC, Clayton South, Melbourne 3169, VIC, Australia

ARTICLE INFO

*Article history:*
Received 27 November 2013
Received in revised form 9 September 2014
Accepted 18 September 2014
Available online 7 October 2014

*Keywords:*
High amylose maize starch
NMR
Dynamic vapour sorption
Digestibility
Dynamics

ABSTRACT

The particle size, water sorption properties and molecular mobility of high amylose maize starch (HAMS) and high amylose maize starch acylated with acetate (HAMSA), propionate (HAMSP) and butyrate (HAMSB) were investigated. Acylation increased the mean particle size ($D_{4,3}$) and lowered the specific gravity ($G$) of the starch granules with an inverse relationship between the length of the fatty acid chain and particle size. Acylation of HAMS with fatty acids lowered the monolayer moisture content with the trend being HAMSB < HAMSA < HAMSP < HAMS, showing that the decrease is affected by factors other than the length of the fatty acid chain. Measurement of molecular mobility of the starch granules by NMR spectroscopy with Carr–Purcell–Meiboom–Gill (CMPG) experiments showed that $T_2$ long was reduced in acylated starches and that drying and storage of the starch granules further reduced $T_2$ long. Analysis of the Free Induction Decay (FID) focussing on the short components of $T_2$ (correlated to the solid matrix), indicated that drying and subsequent storage resulted in alterations of starch at $0.33a_w$ and that these changes were reduced with acylation. *In vitro* enzymatic digestibility of heated starch dispersions by bacterial α-amylase was increased by acylation (HAMS < HAMSB < HAMSP ≤ HAMSA) showing that the trend was not related to the length of the fatty acid chain. Digestibility was enhanced with an increase in particle size, or decrease in $G$, and inversely proportional to the total $T_2$ signal. It is suggested that both external surface area and an internal network of pores and channels collectively influence the digestibility of starch.



## 1. Introduction

As a major source of energy for humans and animals, starch that is used in the production of food products and animal feed is often supplied in its dehydrated form to prevent spoilage during transport. High amylose maize starch (HAMS) and high amylose maize starch acylated with acetate (HAMSA), propionate (HAMSP) and butyrate (HAMSB) increase degradative resistance by mammalian enzymes and help to deliver health promoting short chain fatty acid (SCFA) to the host gut (Clarke et al., 2011). To understand the metabolism of the starches by gut microbiota, we previously investigated the breakdown of HAMS and the three modified HAMS by monocultures of bifidobacteria, ruminococcus and faecalibacteria. The starches were differentially degraded with HAMSA being readily degraded while HAMS and HAMSB the least (Lim et al., 2014a). This trend is consistent with the notion that the butyl group of HAMSB lies parallel to the glucosyl units whereas the acetyl group of HAMSA lie perpendicular (Lopez-Rubio, Clarke, Ben, Topping, & Gilbert, 2009), thus making HAMSA more open and accessible by enzymes. Similar packing was implied in investigations of the hydrodynamic radii of solubilised fractions for these same four starches (Lim et al., 2014b). While starch structural properties are widely acknowledged to be associated with starch digestion, processing, stability and storage (Chanvrier et al.,

*Abbreviations:* $a_w$, Water activity; CPMG, Carr–Purcell–Meiboom–Gill; $D_{4,3}$, mean particle size; DS, degree of substitution; EMC, equilibrium moisture content; G, specific gravity; DVS, dynamic vapour sorption; FID, free induction decay; HAMS, high amylose maize starch; HAMSA, acetylated high amylose maize starch; HAMSP, propionated high amylose maize starch; HAMSB, butyrylated high amylose maize starch; $M_o$, monolayer moisture content; $T_2$, spin–spin relaxation time; $T_1$, spin-lattice relaxation time.

* Corresponding author at: Department of Biochemistry and Molecular Biology, The University of Melbourne, Parkville, Melbourne 3010, VIC, Australia.
Tel.: +61 3 834 42273.
*E-mail address:* prg@unimelb.edu.au (P.R. Gooley).

http://dx.doi.org/10.1016/j.carbpol.2014.09.068
0144-8617/

2007; Shrestha et al., 2012; Zhou, Chung, Kim, & Lim, 2013), this area generally remains understudied particularly for high amylose esterified starches.

Techniques such as Fourier transform infrared spectroscopy, neutron scattering, dynamic vapour sorption (DVS), differential scanning calorimetry and nuclear magnetic resonance (NMR) spectroscopy have been used to elucidate the physio-chemical properties of starch and the role and behaviour of water in food (Choi & Kerr, 2003; Enrione, Hill, & Mitchell, 2007; Zeng, Li, Gao, & Ru, 2011). Factors such as the composition of the starch, treatments applied during food processing and conditions of storage, all impact on the interactions between water and the starch molecules (Åkerberg, Liljeberg, & Björck, 1998; Lewicki, 2004; Svihus, Uhlen, & Harstad, 2005). The interactions between water and biopolymer molecules such as starch have a significant influence on biopolymer functionality (Hermansson & Svegmark, 1996). Despite extensive knowledge about the fundamental properties of starch, the ability to predict starch interactions and functionality remain a challenge to the food and starch industry (Copeland, Blazek, Salman, & Tang, 2009).

In this study, HAMS and the three acylated HAMS were examined to assess the impact that acylation has on specific gravity ($G$), particle size and the effect of dry heat treatment and storage on water sorption in the starch molecules. Additionally, we examined the *in vitro* enzymatic digestibility of heated starch dispersions by bacterial α-amylase. The interactions between starch and water were examined using DVS and water mobility was assessed by $T_2$ distribution profiles using $^1$H NMR spectroscopy using both Carr–Purcell–Meiboom–Gill (CPMG) and Free Induction Decay (FID) investigations. The relationship between particle size and water–starch interactions on the enzymatic digestibility of starch was assessed.

## 2. Materials and methods

### 2.1. Starch material

HAMS, produced by Ingredion (New Jersey, USA) is an unmodified maize starch that contains approximately 70% amylose. HAMS was used as the base starch to manufacture HAMSA, HAMSP and HAMSB (Ingredion). The extent of acylation of these raw starches is expressed as a degree of substitution (DS), which can be defined as the average number of substitution groups per anhydroglucose unit in starch. DS can be calculated using the following equation:

$$\mathrm{DS} = \frac{[S]}{[B]}$$

where $[S]$ is the concentration of the substituent in the sample and $[B]$ is the concentration of the backbone in monomeric terms. As there are only three hydroxyl groups per glucose unit, the maximum DS value for starch is three. The DS values of HAMSA, HAMSP and HAMSB used in this study are 0.22, 0.20 and 0.20, respectively, as determined by Ingredion. The initial moisture content (% dry basis) of the raw starches range from 10.23 to 11.62%.

### 2.2. Amylose content

The amylose content of the raw starches were determined by their iodine binding capacity using a modified ampero-metric method (Gerard, Barron, Colonna, & Planchot, 2001; Larson, Gilles, & Jenness, 1953). 100 mg (±10%) of dry starch was solubilised in 3 ml of 1 N KOH for 10 h at 4 °C with occasional mixing. 3 ml of 1 N HCl and 2 ml of $H_2O$ was added to neutralise the starch solution. 1 ml samples containing diluted starch in the range of 0.5–1 mg and 100 μl of iodine solution (Grams Iodine, Sigma–Aldrich) was prepared and their optical density at 620 nm measured. The amylose content was determined against a standard curve of pure amylose (soluble starch, Sigma Aldrich).

### 2.3. Scanning electron microscopy

The morphology of the dried starch samples were examined using a field emission scanning electron microscope (SEM) (Quanta; Fei Company, Hillsboro, Oregon, U.S.A.) at 10 kV. Raw starch powders were mounted on a stud and coated with gold prior to SEM examination. The detectors used for the SEM observation were an Everhart Thornley detector.

### 2.4. Size distribution and specific gravities

Particle size analysis of the raw starches was measured by light scattering using a Malvern Mastersizer 2000 (Malvern Instrument, Malvern, UK). Raw starch granules were dispersed in $H_2O$ (10% w/v) and added into the apparatus circulating cell stirring at 2000 rpm. A general purpose analysis model within the Mastersizer analysis software was used with particle refractive and absorption indices of 1.53 and 0.1, respectively, while the refractive index of water as the dispersant was 1.33. Duplicate measurements were carried out for each of the starch preparations. Particle size were obtained and expressed in terms of the mean particle size, $D_{4,3}$.

The $G$ (mass density of solids to that of water), of the starches was obtained using a 25 ml density bottle (pycnometer) at 25 °C. 2000 mg (±10%) of raw starch was used in the determination with dd$H_2O$ as solvent.

### 2.5. Dynamic vapour sorption

Vapour sorption properties of the raw starches were determined at 25 °C using a controlled-atmosphere microbalance (Dynamic Vapour Sorption Series 2000, Surface Measurement System Ltd., London, U.K.) housed in a controlled temperature incubator (±0.1 °C) as described previously (Ying et al., 2010). Briefly, a sample (~50 mg) was loaded onto a quartz DVS flat bottom sample pan and pre-equilibrated at 0% RH in a continuous flow of dry air for 1000 min before the sample was ramped to the desired water activity. The mass at the end of this step was used as the dry mass. The sample was then exposed to the following water activity ($a_w$) (0.05, 0.10, 0.20, 0.30, 0.40, 0.50, 0.60, 0.70, 0.80 and 0.90) using a special automatic operation method with d$m$/d$t$ (change in mass/time) mode. The d$m$/d$t$ criterion was set at 0.001% for five consecutive minutes and the maximum amount of time at each $a_w$ was set at 500 min. The changes in sample mass as a function of time were recorded by the microbalance. Using this method, equilibrium moisture content (EMC) at each $a_w$ was determined. The monolayer moisture content ($M_o$) was obtained by fitting the isotherm with Guggenheim–Anderson–De Boer model as previously described (Ying et al., 2010). The moisture isotherm was calculated using DVS Analysis Macro version 6.1. The error of the duplicated sorption isotherms was within 3%.

### 2.6. NMR spectroscopy

Raw starch samples (non-dried) were placed in glass tubes and equilibrated at $a_w$ 0.33 and 0.70 using saturated solutions of magnesium chloride ($MgCl_2$) or of strontium chloride ($SrCl_2$) in sealed glass desiccators. Additionally, dried raw starch samples were prepared similarly following drying at 100 °C for 2 h. Spin–spin relaxation time ($T_2$) were obtained on a MARAN ULTRA 23 MHz spectrometer (Oxford Instruments, Oxfordshire) using the CPMG technique (Hoobin et al., 2013). The 90°–180° pulse spacing ($\tau$) in the CPMG sequence was set to 30 μs and a dwell time of

**Table 1**
Specific gravity and % amylose of HAMS, HAMSA, HAMSP and HAMSB.

| Starch | HAMS | HAMSA | HAMSP | HAMSB |
|---|---|---|---|---|
| Specific gravity | 1.50 (0.01) | 1.40 (0.03) | 1.40 (0.01) | 1.44 (0.02) |
| % Amylose | 70.81 (1.20) | 69.33 (1.16) | 70.56 (1.63) | 69.47 (0.89) |

The specific gravity and % amylose of high amylose maize starch (HAMS), acetylated high amylose maize starch (HAMSA), propionated high amylose maize starch (HAMSP) and butyrylated high amylose maize starch (HAMSB) were determined in triplicate. (±SEM).

0.5 μs and collected until the signal decayed to baseline. The number of scans used was 32 or 64, selected so that the signal to noise ratio was sufficient. Data were fitted using a double exponential equation in Wavemetrics (Igor) software and obtaining two $T_2$ time constants. After storage for 6 months in $a_w$ 0.33 and 0.7, additional analysis of the shorter components (correlated to the solid matrix) was carried out using the FID. The FID investigation improved the determination of the shorter $T_2$ component, which could not be observed accurately using the CPMG method.

### 2.7. Enzymatic digestion by amylase

All starch samples were dispersed in water (0.625% w/v), aliquot into 8 ml fractions and autoclaved for 15 min at 121 °C. Amylase stock solution (α-amylase from *Bacillus licheniformis*, Sigma-Aldrich) was added to each fraction to make up a final volume of 10 ml, a final enzymatic concentration of 50 U/ml and 0.5% (w/v) starch and incubated at 37 °C for the duration of the experiment. To quantify residual starch, the sample is centrifuged at 4000 × *g* for 5 min. The pelleted starch is hydrolysed using 10% HCl (v/v) at 95 °C and quantified using $^1$H NMR (Lim et al., 2014a).

## 3. Results

### 3.1. Amylose content, shape and size distribution of starch granules

Amylose:amylopectin ratios of the chemically modified starches were not altered significantly by acylation, with the four starches containing 69.33–70.81% amylose (Table 1). All four starches appear similar in size and were generally round or oval with a small percentage being irregular (Fig. 1). The micrographs of HAMS display filamentous and rod-like characteristics typical in starches with high-amylose content (Fishman, Cooke, White, & Damert, 1995). In contrast, modified HAMS granules appear to be more angular, with bulbous protrusions on the starch surfaces.

The particle size distributions of the raw starch obtained by light scattering (Fig. 2) confirms that there was a heterogeneous distribution of particles, with modified HAMS possessing a wider range

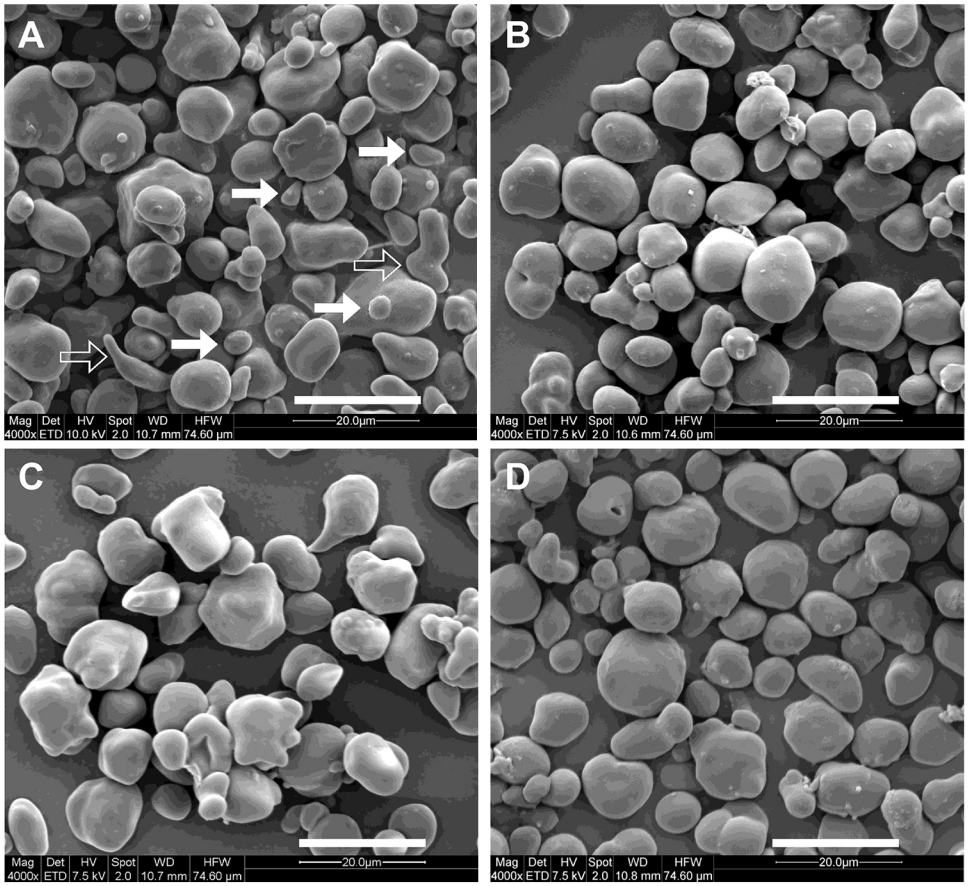


**Fig. 1.** SEM images of (A) HAMS, (B) HAMSA, (C) HAMSP and (D) HAMSB illustrating shape differences and size distributions. Filamentous and rod-like starches are indicated by the open arrows while solid arrows indicate small particles found only in HAMS. Images obtained are of raw starches (prior to dry heat treatment and storage at $a_w$ 0.33 or 0.70). All scale bars = 20 μm.

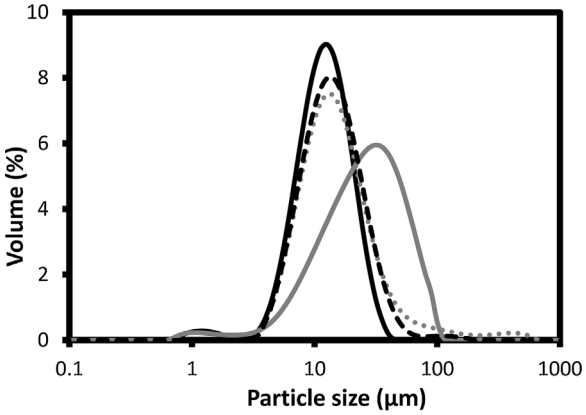


**Fig. 2.** Deconvoluted light scattering data showing particle size distribution of HAMS and modified HAMS. The distributions for raw starch HAMS (black lines), HAMSA (grey lines), HAMSP (broken grey lines) and HAMSB (broken black lines) illustrate larger particle size of HAMSA and significant overlap between HAMS, HAMSP and HAMSB. Duplicate measurements were obtained prior to dry heat treatment and storage at $a_w$ 0.33 or 0.70.

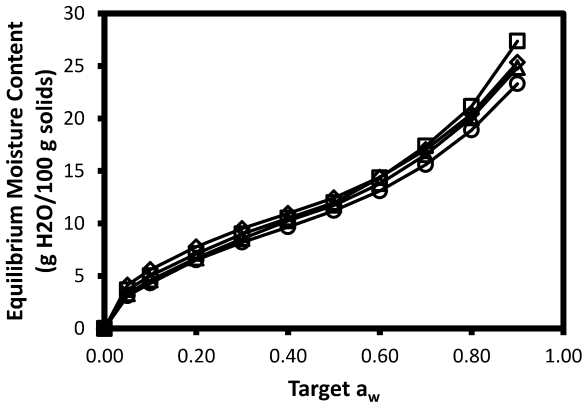


**Fig. 3.** Thermal isotherms of HAMS (◊), HAMSA (□), HAMSP (△) and HAMSB (○) illustrating the water sorption properties of raw starches (prior to dry heat treatment and storage at $a_w$ 0.33 or 0.70). Duplicate measurements were obtained with the error of duplicated isotherms within 3%.

than HAMS, and the most polydispersed starch being HAMSA. The mean particle size ($D_{4,3}$) of HAMS (12.4 μm) and HAMSB (15.8 μm) were found to be smaller than HAMSP (24 μm) and HAMSA (28.7 μm) with the trend being HAMS < HAMSB < HAMSP < HAMSA. Corn starches are typically in the range of 2–26 μm with commercial corn starch having a $D_{4,3}$ of 16.9 μm (Hossen et al., 2011; Vasanthan & Bhatty, 1996).

The polydispersity of modified HAMS, especially HAMSA, suggests a portion of the starch may either be larger due to esterification-induced change or are aggregating. With light scattering, a few large aggregates can skew the distribution towards one that emphasises the size of the large particles. To further investigate other factors that might contribute to the $D_{4,3}$ differences, the $G$ of the starches were measured as this provides insights into esterification-induced alterations to the internal packing of the starch (Table 1). There was no significant difference in $G$ between HAMSA and HAMSP. However, HAMS was found to have the highest $G$, followed by HAMSB and HAMSA/HAMSP. HAMS is the most dense, with the trend in density being HAMSA, HAMSP < HAMSB < HAMS which is consistent with the observed $D_{4,3}$ values.

### 3.2. Dynamic vapour sorption

The moisture sorption isotherms of the starches are given in Fig. 3. The $M_o$ of the starches are in a range of 7.9–8.4 g·$H_2O$/100 g solids with HAMSB (7.9) < HAMSA (8.0) < HAMSP (8.3) < HAMS (8.4), showing that the trend in the decrease in $M_o$ did not parallel the increase in length of the fatty acid chain. The $M_o$ values of HAMS and modified HAMS were lower than reported for potato flour (9.79 g·$H_2O$/100 g solids), wheat flour (9.89 g·$H_2O$/100 g solids) and corn flour (10.27 g·$H_2O$/100 g solids) (Timmermann, Chirife, & Iglesias, 2001).

### 3.3. NMR spectroscopy

The measured $T_2$ distributions show decaying signals representative of both mobile and less mobile $^1H$ components in the samples which provide information on the interactions of water with the starch molecules. The $T_2$ values and distribution of the dried and non-dried starches equilibrated at $a_w$ values of 0.33 and 0.70 after 19 days using the described CPMG sequence (Hoobin et al., 2013) are shown in Fig. 4, respectively. While the exact moisture content are not measured for each sample due to the small sample size, moisture uptake was measured by weight change and is given in Table S1 (see Supplemental material). The distribution curves showed that $T_2$ long is reduced in acylated starches and that drying and subsequent storage of the starch granules further reduced $T_2$ long. As the distribution from the CPMG decay (Fig. 4) does not enable an accurate determination of the $T_2$ short and long values, the original data was processed by Igor software with a double exponential fit to obtain $T_2$ values with better accuracy. Using Igor software two distinct $T_2$ time constants could be discerned (Table 2) which confirms that $T_2$ values and % contributions to the signal were decreased by acylation. At 0.33 $a_w$, a fast-decaying component is characterised with the following $T_2$ short values:

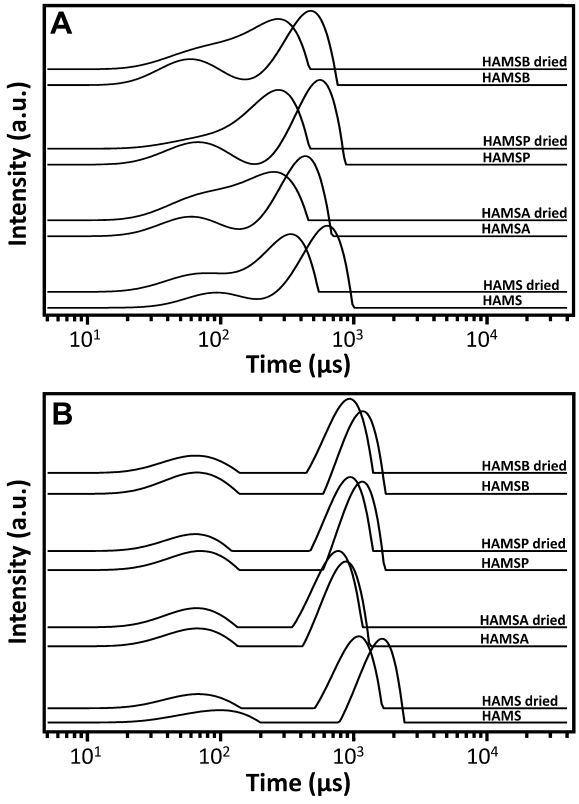


**Fig. 4.** $T_2$ distribution of dried and non-dried HAMS and modified HAMS after 19 days of storage at $a_w$ of (A) 0.33 and (B) 0.7 as obtained using a CPMG sequence. The $y$-dimension is off-set for clarity. Poor resolution of $T_2$ short and $T_2$ long as seen at $a_w$ 0.33 is discussed in-text.

**Table 2**
$T_2$ short and $T_2$ long profiles of dried and non-dried starches after 19 days storage at $a_w$ values of 0.33 and 0.7 using the CPMG decay signal [a].

| $a_w$ 0.33 | | Non-dried | | | | Dried | | | |
|---|---|---|---|---|---|---|---|---|---|
| | | HAMS | HAMSA | HAMSP | HAMSB | HAMS | HAMSA | HAMSP | HAMSB |
| $T_2$ short | Time (μs) | 294 | 73.5 | 112 | 81.4 | 93.0 | 116 | 171 | 128 |
| | % Contribution | 54.3 | 38.1 | 35.4 | 42.1 | 48.8 | 70.6% | 75.5 | 70.0 |
| $T_2$ long | Time (μs) | 814 | 453 | 609 | 512 | 394 | 409 | 484 | 434 |
| | % Contribution | 45.7 | 61.9 | 64.6 | 57.9 | 51.2 | 29.4 | 24.5 | 30.0 |
| $a_w$ 0.70 | Non-dried | | | | Dried | | | | |
| | HAMS | HAMSA | HAMSP | HAMSB | HAMS | HAMSA | HAMSP | HAMSB | |
| $T_2$ short | Time (μs) | 218 | 98.6 | 102 | 96.6 | 192 | 86.6 | 80.2 | 117 |
| | % Contribution | 20.4 | 25.8 | 25.4 | 28.7 | 22.0 | 30.1 | 28.0 | 26.5 |
| $T_2$ long | Time (μs) | 1670 | 890 | 1170 | 1190 | 1150 | 780 | 955 | 969 |
| | % Contribution | 79.6 | 74.2 | 74.6 | 71.3 | 78.0 | 69.9 | 72.0 | 73.5 |

[a] Error is up to 3% of the measured values. For each starch (HAMS, high amylose maize starch; HAMSA, acetylated high amylose maize starch; HAMSP, propionated high amylose maize starch and HAMSB, butyrylated high amylose maize starch), condition (non-dried, dried) and $T_2$ time ($T_2$ short, $T_2$ long), the mean $T_2$, the % contribution to the integral of the total $T_2$ is given.

HAMS (294 μs) > HAMSP (112 μs) > HAMSB (81.4 μs) > HAMSA (73.5 μs). The same trend is observed for the slow-decaying component with the following $T_2$ long values: HAMS (814 μs) > HAMSP (609 μs) > HAMSB (512 μs) > HAMSA (453 μs). At 0.70 $a_w$, these times became less discerning for the acylation state. While the fast-decaying component shows similar values ($T_2$ short) to the 0.33 $a_w$ data: HAMS (218 μs) > [HAMSA ~ HAMSP ~ HAMSB (97–102 μs)], the slow-decaying data showed an increase in $T_2$ values ($T_2$ long): HAMS (1670 μs) > HAMSP~HAMSB (1170–1190 μs) > HAMSA (890 μs). However, in all cases, acylation for the non-dried starches decreases $T_2$ for both fast and slow-decaying components, suggesting a more rigid structure is formed after acylation.

As the CPMG sequence did not allow detection of the very short $T_2$ component (solid matrix), the FID was used to obtain more accurate estimations of these fast-decaying components after 6 month storage (Table 3). The major findings relating to the effects of acylation on molecular mobility in non-dried starches stored at 0.33 $a_w$ were that (i) the integral of the total $T_2$ signal of the FID component was reduced in acylated starches compared to the unmodified starch with the order of the total $T_2$ signal being HAMS > HAMSB > HAMSP > HAMSA and (ii) the contribution of $T_2$ short of the FID component increased with the length of the fatty acid chain, suggesting that as fatty acid length is increased, there are more immobile components. Long term storage of previously dried starch (100 °C/2 h) at $a_w$ 0.33 caused a shift in $T_2$ distribution with reduced $T_2$ long (both contribution and integral value) (Table 3). Furthermore, the % increase in the contribution of $T_2$ short to the total signal was greatest for HAMS. The lower % increase in the contribution of $T_2$ short for the acylated starches on storage is consistent with the mobility of starch being reduced with acylation (Adebowale & Lawal, 2003; Lawal, 2004).

### 3.4. Digestion of heated starch dispersion by α-amylase

Digestion of heated starch dispersion *in vitro* by bacterial α-amylase was tracked over a time period of 27 h as shown in Fig. 5. Heated starch dispersions adopt a 'burst granule' state with a fraction being solubilised and the largest of these burst granules being visible to the naked eye as grainy particulates. The hydrodynamic radii of solubilised starch have been shown to follow a trend where HAMSA > HAMSP > HAMSB > HAMS (Lim et al., 2014b). In the digestion of heated starch dispersions, a similar trend is observed with the order of most rapid to least digested starch determined to be: HAMSA ≥ HAMSP > HAMSB > HAMS. This trend was also observed in a study of acylated high amylose maize starch digestibility by probiotics and gut bacterial species (Lim et al., 2014a).

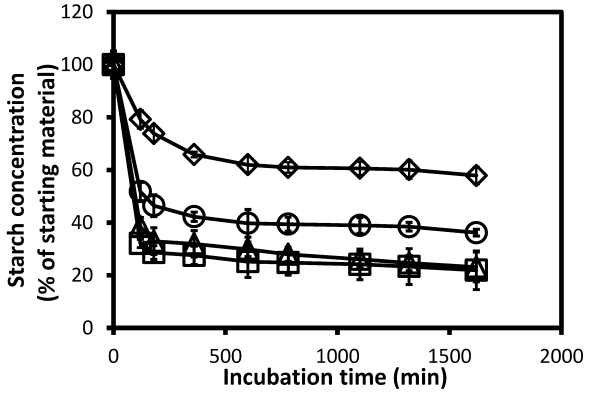


**Fig. 5.** Digestion of HAMS (◊), HAMSA (□), HAMSP (△) and HAMSB (○) by α-amylase as a function of starting concentration. Error bars represent ±SEM of four independent measurements.

## 4. Discussion

Four starches (HAMS, HAMSA, HAMSP and HAMSB) were examined by various techniques to understand their physical characteristics (SEM, *G*, mean particle sizing), water–starch interactions (DVS and $^1$H NMR spectroscopy) and their relationship to starch digestibility and mobility during storage.

### 4.1. Acylation and mean particle size

Increase in angular and irregular granules was observed post-acylation, with the loss of filamentous and rod-like characteristics. The proportion of rod-like granules was previously determined to correlate with amylose content (Fishman et al., 1995; Jiang et al., 2010), although this was not observed in the current study. The bulbous surface of angular granules in modified HAMS also appears to be formed through fusion of smaller granules, as previously observed by (Jiang et al., 2010), which may contribute to the increase in particle size.

Acylation increased the mean particle size with HAMS < HAMSB < HAMP < HAMSA, showing an inverse relationship between acylated group length and particle size. The lack of a direct relationship between the length of the fatty acid chain is contrary to expectations. However, our finding may be rationalised by observations of starch structure from X-ray diffraction studies (Lopez-Rubio et al., 2009), which inferred that acylation introduced void spaces in the starch structure. Additionally, longer chain fatty acids (butyric acid) results in smaller void spaces while shorter fatty acids such as acetic acid results in more pronounced structural

**Table 3**
$T_2$ short and $T_2$ long profiles of dried and non-dried starches after 6 months of equilibration at $a_w$ values of 0.33 and 0.70 using the FID[a].

| $a_w$ 0.33 | | Non-dried | | | | Dried | | | |
|---|---|---|---|---|---|---|---|---|---|
| | | HAMS | HAMSA | HAMSP | HAMSB | HAMS | HAMSA | HAMSP | HAMSB |
| $T_2$ short | Time (μs) | 11.2 | 12.1 | 12.1 | 12.1 | 11.2 | 11.7 | 11.7 | 12.1 |
| | Integral (a.u.) | 65,625 | 60,514 | 65,839 | 68,519 | 64,454 | 64,508 | 67,809 | 71,127 |
| | % Contribution | 80.8 | 82.3 | 83.2 | 85.0 | 84.8 | 86.0 | 86.9 | 88.1 |
| $T_2$ long | Time (μs) | 517 | 536 | 642 | 597 | 360 | 387 | 388 | 387 |
| | Integral (a.u) | 15,638 | 12,975 | 13,340 | 12,102 | 11,541 | 10,532 | 10,187 | 9630 |
| | % Contribution | 19.2 | 17.7 | 16.8 | 15.0 | 15.2 | 14.0 | 13.1 | 11.9 |
| $T_2$ total | Total integral | 81,263 | 73,489 | 79,179 | 80,621 | 75,995 | 75,040 | 77,996 | 80,757 |
| $a_w$ 0.70 | Non-dried | | | | Dried | | | | |
| | HAMS | HAMSA | HAMSP | HAMSB | HAMS | HAMSA | HAMSP | HAMSB | |
| $T_2$ short | Time (μs) | 10.1 | 10.9 | 11.3 | 11.7 | 10.1 | 10.9 | 10.9 | 11.7 |
| | Integral (a.u.) | 60,345 | 58,673 | 62,527 | 66,128 | 58,140 | 57,322 | 60,743 | 67,837 |
| | % Contribution | 70.1 | 69.5 | 71.5 | 73.7 | 71.3 | 70.0 | 73.0 | 74.7 |
| $T_2$ long | Time (μs) | 666 | 620 | 691 | 691 | 642 | 598 | 666 | 666 |
| | Integral (a.u.) | 25,763 | 25,770 | 24,863 | 23,607 | 23,347 | 24,600 | 22,507 | 22,943 |
| | % Contribution | 29.9 | 30.5 | 28.5 | 26.3 | 28.7 | 30.0 | 27.0 | 25.3 |
| $T_2$ total | Total integral | 86,108 | 84,443 | 87,390 | 89,735 | 81,487 | 81,922 | 83,250 | 90,780 |

[a] Error is up to 3% of the measured values. For each starch (HAMS, high amylose maize starch; HAMSA, acetylated high amylose maize starch; HAMSP, propionated high amylose maize starch and HAMSB, butyrylated high amylose maize starch), condition (non-dried, dried) and $T_2$ time ($T_2$ short, $T_2$ long), the mean $T_2$, the integral attributed to that $T_2$ and % contribution to the integral of the total $T_2$ is given.

changes and larger void spaces (Lopez-Rubio et al., 2009). This is due to longer chain fatty acids being able to lie parallel to the starch backbone due to their length and flexibility. Comparatively, short fatty acids such as acetic acid extend perpendicular to the starch backbone resulting in greater disruptions to the semi-crystalline nature of starch granules (Lopez-Rubio et al., 2009). Support for alteration in internal packing and introduction of void spaces within modified HAMS is also evident in the G of the four starches (Table 1).

### 4.2. Starch alterations on storage

Drying of starch at 100 °C altered starch-moisture interactions, as evidenced by the changed NMR profiles on starches that had been pre-exposed to heat (100 °C/2 h) before storage at various $a_w$, using both the CPMG and FID. Using the CPMG sequence, the dried starches had shorter $T_2$ long illustrating an impeded ability for water to interact with the starch components (Fig. 4, Table 2), an effect that is evident after six months. This effect is most pronounced in HAMS while modified HAMS was affected to a lesser degree, suggesting that acylation reduces mobility changes on storage. Confirmation that mobility was reduced in acylated starches was obtained with the FID investigation (Table 3). Others have shown that chemical modification through cross-linking (Liu, Ramsden, & Corke, 1999) and acylation of starch alters its mobility and decreases retrogradation (Adebowale & Lawal, 2003; Lawal, 2004).

### 4.3. Relationships between physio-chemical properties and factors affecting starch digestibility

The interaction between water and starch, measured by DVS and NMR are related. The equilibrium water content (EMC) (Fig. 3) and $T_2$ long (Table 3) are linearly related (but not significantly; Pearson correlation = 0.938, $P$-value = 0.062) (Fig. 6A), but not the multilayer water content (EMC less $M_o$) (Pearson correlation = −0.693, $P$-value = 0.307) (Fig. 6B). $T_2$ long has been previously found to be correlated to multilayer water and inactivation rates of encapsulated bacteria (Hoobin et al., 2013; Ying et al., 2010). A similar correlation is not observed in HAMS and modified HAMS, possibly due to the heterogenous structure of starch and differences in particle sizing impeding a straightforward model of water interaction. In this work, HAMSA, which has the largest mean particle size and total $T_2$ signal, had the greatest digestibility followed by HAMSP, HAMSB and HAMS, respectively.

The relationship between the measured physio-chemical properties (i.e. particle size and water relations) and starch digestibility in disrupted granules is complex. Others have found that amylase digestion of starch was reduced as particle size of starch granules was increased (Dhital, Shrestha, & Gidley, 2010). They further suggested that digestion rate was essentially determined by external-surface area for potato starch. However, in maize starch,

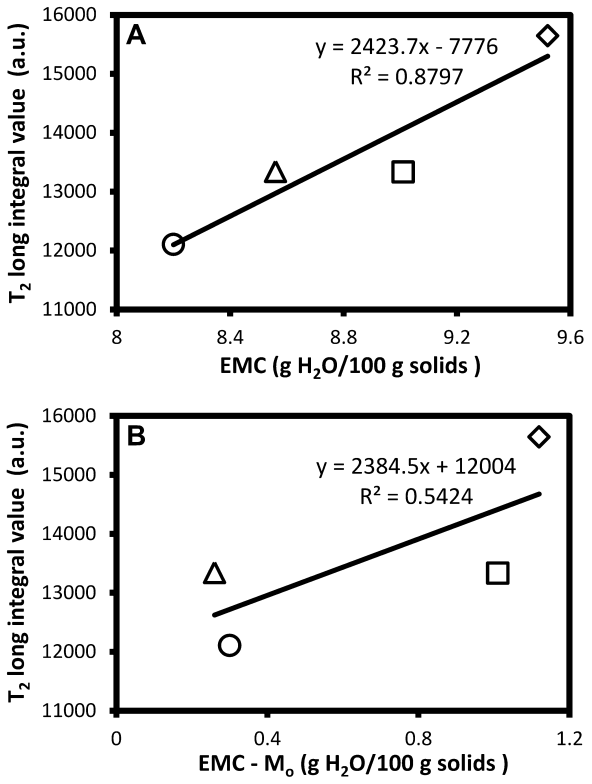


**Fig. 6.** Correlation between $T_2$ long integral value and (A) equilibrium moisture content and (B) equilibrium moisture content less monolayer moisture content at $a_w$ of 0.33 for HAMS (◊), HAMSA (□), HAMSP (△) and HAMSB (○).

digestibility is often larger than predicted from external surface area, due to the contribution of surface pores and channels to the effective total surface area (Dhital et al., 2010).

The observed effects of particle size and the lack of correlation of mobile water (long $T_2$) or fatty acid chain length with starch digestion, suggests that other factors have a more significant influence on digestibility of acylated starches. This lack of correlation between fatty acid chain length (i.e. hydrophobicity) is contradictory to studies in α-amylose fragments, which found both glycosidic linkage conformation and hydrophobicity to be equal factors in water sorption (Fringant, Tvaroska, Mazeau, Rinaudo, & Desbrieres, 1995). It is suggested that the disruption to the starch structure caused by the introduction of various fatty acids, as previously observed by others using small angle x-ray scattering (Lopez-Rubio et al., 2009), possibly has the overriding influence on the digestibility of the starch.

## 5. Conclusion

Moisture is an inherent component of many food materials with an important role in the prediction of material properties and food shelf life. Our study shows that acylation with short chain fatty acids alter the physical and chemical properties of starch, though not in accordance to the length of the hydrophobic alkyl chain. Other factors such as openness of the internal structure play a pivotal role. DVS and NMR spectroscopy are valuable tools in understanding starch behaviour and properties in food processing. While heat induced changes and hydrophobicity of acyl chains are contributory, structural alteration appears as the overriding factor affecting acylated starch properties. Systemic studies on other food material are required to determine if this observation extends to other dehydrated material. Importantly, current findings suggest that while butylation of HAMS may aid in delivery of butyric acid to the lower gut (Clarke et al., 2011), the structural packing of HAMSB is not optimal for bacterial degradation. In contrast, HAMSA adopts a more open structure and is more readily digested suggesting that mixed acylation may produce a more accessible starch that will better function as a delivery vehicle for butyrate.

## Acknowledgements

We thank Dr Julie Clarke and Ben Scherer of CSIRO Animal Food and Health Sciences (Adelaide, Australia) for the provision of starches, Sukhdeep Bhail for particle size analysis and Lydia Ong for scanning electron microscopy assistance. The research presented is supported in part by a CSIRO OCE Postgraduate Scholarship and University of Melbourne MIFRS Scholarship.

## Appendix A. Supplementary data

Supplementary data associated with this article can be found, in the online version, at http://dx.doi.org/10.1016/j.carbpol.2014.09.068.

## References

Adebowale, K. O., & Lawal, O. S. (2003). Functional properties and retrogradation behaviour of native and chemically modified starch of mucuna bean (*Mucuna pruriens*). *Journal of the Science of Food and Agriculture*, *83*(15), 1541–1546.

Åkerberg, A., Liljeberg, H., & Björck, I. (1998). Effects of amylose/amylopectin ratio and baking conditions on resistant starch formation and glycaemic indices. *Journal of Cereal Science*, *28*(1), 71–80.

Chanvrier, H., Uthayakumaran, S., Appelqvist, I. A. M., Gidley, M. J., Gilbert, E. P., & Lopez-Rubio, A. (2007). Influence of storage conditions on the structure, thermal behavior, and formation of enzyme-resistant starch in extruded starches. *Journal of Agricultural and Food Chemistry*, *55*(24), 9883–9890.

Choi, S.-G., & Kerr, W. L. (2003). 1H NMR studies of molecular mobility in wheat starch. *Food Research International*, *36*(4), 341–348.

Clarke, J. M., Topping, D. L., Christophersen, C. T., Bird, A. R., Lange, K., Saunders, I., et al. (2011). Butyrate esterified to starch is released in the human gastrointestinal tract. *American Journal of Clinical Nutrition*, *94*(5), 1276–1283.

Copeland, L., Blazek, J., Salman, H., & Tang, M. C. (2009). Form and functionality of starch. *Food Hydrocolloids*, *23*(6), 1527–1534.

Dhital, S., Shrestha, A. K., & Gidley, M. J. (2010). Relationship between granule size and in vitro digestibility of maize and potato starches. *Carbohydrate Polymers*, *82*(2), 480–488.

Enrione, J. I., Hill, S. E., & Mitchell, J. R. (2007). Sorption behavior of mixtures of glycerol and starch. *Journal of Agricultural and Food Chemistry*, *55*(8), 2956–2963.

Fishman, M. L., Cooke, P., White, B., & Damert, W. (1995). Size distributions of amylose and amylopectin solubilized from corn starch granules. *Carbohydrate Polymers*, *26*(4), 245–253.

Fringant, C., Tvaroska, I., Mazeau, K., Rinaudo, M., & Desbrieres, J. (1995). Hydration of alpha-maltose and amylose: Molecular modelling and thermodynamics study. *Carbohydrate Research*, *278*(1), 27–41.

Gerard, C., Barron, C., Colonna, P., & Planchot, V. (2001). Amylose determination in genetically modified starches. *Carbohydrate Polymers*, *44*(1), 19–27.

Hermansson, A.-M., & Svegmark, K. (1996). Developments in the understanding of starch functionality. *Trends in Food Science and Technology*, *7*(11), 345–353.

Hoobin, P., Burgar, I., Zhu, S., Ying, D., Sanguansri, L., & Augustin, M. A. (2013). Water sorption properties, molecular mobility and probiotic survival in freeze dried protein–carbohydrate matrices. *Food and Function*, *4*(9), 1376–1386.

Hossen, M. S., Sotome, I., Takenaka, M., Isobe, S., Nakajima, M., & Okadome, H. (2011). Effect of particle size of different crop starches and their flours on pasting properties. *Japan Journal of Food Engineering*, *12*(1), 29–35.

Jiang, H., Horner, H. T., Pepper, T. M., Blanco, M., Campbell, M., & Jane, J.-l. (2010). Formation of elongated starch granules in high-amylose maize. *Carbohydrate Polymers*, *80*(2), 533–538.

Larson, B. L., Gilles, K. A., & Jenness, R. (1953). Amperometric method for determining sorption of iodine by starch. *Analytical Chemistry*, *25*(5), 802–804.

Lawal, O. S. (2004). Succinyl and acetyl starch derivatives of a hybrid maize: Physicochemical characteristics and retrogradation properties monitored by differential scanning calorimetry. *Carbohydrate Research*, *339*(16), 2673–2682.

Lewicki, P. P. (2004). Water as the determinant of food engineering properties. A review. *Journal of Food Engineering*, *61*(4), 483–495.

Lim, Y. M., Barnes, M. B., Gras, S. L., McSweeney, C., Lockett, T., Augustin, M. A., et al. (2014). Esterification of high amylose starch with short chain fatty acids modulates degradation by Bifidobacterium spp. *Journal of Functional Foods*, *6*, 137–146.

Lim, Y. M., Yao, S., Gras, S. L., McSweeney, C., Lockett, T., Augustin, M. A., et al. (2014). Hydrodynamic radii of solubilized high amylose native and modified starches by pulsed field gradient NMR diffusion measurements. *Food Hydrocolloids*, *40*, 16–21.

Liu, H., Ramsden, L., & Corke, H. (1999). Physical properties of cross-linked and acetylated normal and waxy rice starch. *Starch-Stärke*, *51*(7), 249–252.

Lopez-Rubio, A., Clarke, J. M., Ben, S., Topping, D. L., & Gilbert, E. P. (2009). Structural modifications of granular starch upon acylation with short-chain fatty acids. *Food Hydrocolloids*, *23*(7), 1940–1946.

Shrestha, A. K., Blazek, J., Flanagan, B. M., Dhital, S., Larroque, O., Morell, M. K., et al. (2012). Molecular, mesoscopic and microscopic structure evolution during amylase digestion of maize starch granules. *Carbohydrate Polymers*, *90*(1), 23–33.

Svihus, B., Uhlen, A. K., & Harstad, O. M. (2005). Effect of starch granule structure, associated components and processing on nutritive value of cereal starch: A review. *Animal Feed Science and Technology*, *122*(3-4), 303–320.

Timmermann, E. O., Chirife, J., & Iglesias, H. A. (2001). Water sorption isotherms of foods and foodstuffs: BET or GAB parameters? *Journal of Food Engineering*, *48*(1), 19–31.

Vasanthan, T., & Bhatty, R. S. (1996). Physicochemical properties of small- and large-granule starches of waxy, regular, and high-amylose Barleys. *Cereal Chemistry*, *73*(2), 199–207.

Ying, D. Y., Phoon, M. C., Sanguansri, L., Weerakkody, R., Burgar, I., & Augustin, M. A. (2010). Microencapsulated *Lactobacillus rhamnosus* GG powders: Relationship of powder physical properties to probiotic survival during storage. *Journal of Food Science*, *75*(9), E588–E595.

Zeng, J., Li, G., Gao, H., & Ru, Z. (2011). Comparison of A and B starch granules from three wheat varieties. *Molecules*, *16*(12), 10570–10591.

Zhou, X., Chung, H.-J., Kim, J.-Y., & Lim, S.-T. (2013). In vitro analyses of resistant starch in retrograded waxy and normal corn starches. *International Journal of Biological Macromolecules*, *55*, 113–117.